

Coupled micro-resonators for second-order integrated nonlinear optics

Yannick Dumeige*

Université de Rennes, ENSSAT, CNRS, Institut FOTON-UMR 6082, 6 rue de Kerampont, 22300 Lannion, France

Yoan Léger

Université de Rennes, INSA Rennes, CNRS, Institut FOTON-UMR 6082, F-35000 Rennes, France

(Dated: June 19, 2025)

We investigate second-order nonlinear processes in a system of two coupled identical optical micro-resonators. The double resonance and phase-matching conditions are simultaneously obtained thanks to the frequency splitting induced by the resonator coupling. The analysis made in the framework of the coupled mode theory is applied to the second harmonic generation process in two whispering gallery mode microdisks made in III-V materials.

Keywords: Second harmonic generation, phase-matching, coupled resonators, whispering gallery mode resonators

Optical micro-resonators are of great interest for nonlinear photonics since they enable simultaneously, high integration, low power operation and high stability [1]. One of the most striking applications based on third-order nonlinear optics in micro-resonators is the integration of frequency comb sources on a chip [2]. Second-order nonlinear optics can also take benefit from the use of optical micro-resonators which could lead to the miniaturization of frequency converters, optical parametric oscillators or entangled photon sources [3]. In this aim, the platform of III-V semiconductors is promising since they have high second-order susceptibilities, high refractive index and direct band gap which let envisage micro- or nano-photonics nonlinear or quantum active devices [4] in a wide spectral band. Considering GaP for instance, the transparency domain ranges from $0.55 \mu\text{m}$ to $11 \mu\text{m}$ [5] up to wavelength inaccessible to lithium niobate. III-V materials are isotropic, thus birefringence phase matching is not possible and several methods have been demonstrated to circumvent this issue [6–10]. In this context, natural quasi-phase matching in semiconductor whispering gallery mode (WGM) resonators have been proposed [11, 12] and experimentally demonstrated [13]. Nevertheless, due to the very high dispersion of III-V semiconductors, practical implementations of this quasi-phase matching scheme also rely on the use of modal phase matching [14–16] reducing the effective nonlinear susceptibility due to a low interacting fields overlap. Furthermore, complex numerical techniques can be implemented to optimize the phase matching and the nonlinear overlap in the design of doubly resonant nonlinear photonic structures [17–19]. From another point of view, it has been shown that the coupling of several resonators or of counter-propagating modes within a single resonator allows the control or the engineering of the dispersion in $\chi^{(3)}$ processes [20–22]. Coupled resonator structures can be used to reach functionalities which are not attainable with single nonlinear resonators [23]. If we restrict our-

selves to the case of second-order effects, only few works have been devoted to the coupling of nonlinear micro-resonators [24–26]. In particular, it has been shown in the tight binding approximation that the dispersion induced by the weak coupling of resonators can be used to reach the phase matching condition for SHG in a long chain of $\chi^{(2)}$ microcavities [24].

In this paper, we propose a simple and comprehensive design method using the unique properties of the coupling between two identical WGM resonators to obtain the phase matching condition. Using a benchmark of GaP WGM microdisks, we show that the strong coupling between two resonators helps to reach the natural quasi-phase matching condition with low radial order modes in the process of second harmonic generation (SHG). This approach would lead to reach the low-power high-conversion regime on a chip.

Figure 1 is a sketch of the structure studied in this paper. It consists of two rings or disks of radius $R = L/\pi$ mutually coupled due to the overlap of the evanescent part of their modes. The resonators are coupled to two insertion and extraction waveguides with the same rate. The curvilinear abscissa along the resonator is called s . The fundamental (F) fields are denoted $A_i(s) = \mathcal{A}_i(s)e^{j(\omega t - \beta_1 s)}$ and the second harmonic (SH) fields $B_i(s) = \mathcal{B}_i(s)e^{j(2\omega t - \beta_2 s)}$ with $i \in [1, 8]_{\mathbb{N}}$ and where $\beta_1(\omega)$ and $\beta_2(2\omega)$ are respectively the propagation constants of the F and SF modes whose angular frequencies are respectively ω and 2ω . k_i and t_i are the coupling and transmission coefficients (with $|k_i|^2 + |t_i|^2 = 1$) between the guides and the resonators, we can write the corresponding coupling matrices [27]

$$M_i = \begin{pmatrix} t_i & k_i \\ -k_i^* & t_i^* \end{pmatrix} \quad (1)$$

where $i = 1$ for the F field and $i = 2$ for the SH field. The coupling between the two resonators is described by two coefficients κ_i and τ_i (with also $|\kappa_i|^2 + |\tau_i|^2 = 1$) and thus by the matrix

$$P_i = \begin{pmatrix} \tau_i & \kappa_i \\ -\kappa_i^* & \tau_i^* \end{pmatrix}. \quad (2)$$

* yannick.dumeige@univ-rennes.fr

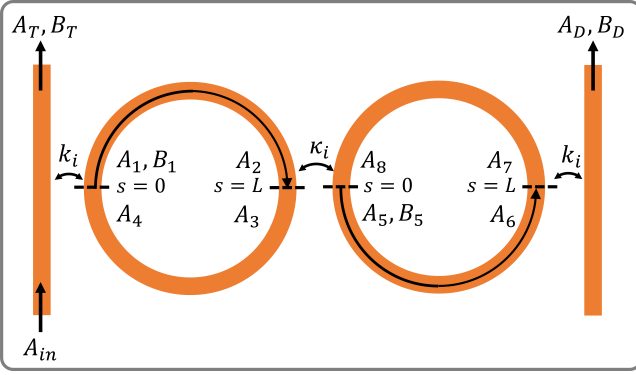


FIG. 1. System of coupled ring or disk resonators of perimeter $2L$. A_i and B_i are the F and SH mode amplitudes within the structure. k_i are the coupling between the access bus waveguides and the structure. κ_i are the coupling coefficient between the two resonators. A_{in} is the input F mode amplitude. A_T and B_T are the F and SH output mode amplitude on the trough port. A_D and B_D are the output mode amplitude on the drop port.

We have for instance $(A_T \ A_1)^T = M_1(A_{in} \ A_4)^T$, $(B_D \ B_7)^T = M_2(0 \ B_6)^T$ and $(A_3 \ A_5)^T = P_1(A_2 \ A_8)^T$. We consider that the pump is undepleted and thus all the calculations are linear for the F fields. Using the matrices M_1 and P_1 it is straightforward to calculate the field $A_i(s)$ at each point of the system [23]. In the case of zinc-blende symmetry materials such as GaP, the second-order nonlinear susceptibility depends on s in the form $\chi^{(2)}(s) = \chi_{0+}^{(2)}e^{j\frac{2s}{R}} + \chi_{0-}^{(2)}e^{-j\frac{2s}{R}}$ [11, 28]. The SH field is then calculated along each half perimeter of the resonator by integrating the following equation

$$\frac{dB_{2p+1}}{ds} = A_{2p+1}^2(s_0) \left(\chi_{0+}^{(2)}e^{j\frac{2s}{R}} + \chi_{0-}^{(2)}e^{-j\frac{2s}{R}} \right) e^{j\Delta\beta s} \quad (3)$$

for $p \in [0, 3]_{\mathbb{N}}$ with $\Delta\beta = \beta_2 - 2\beta_1$; $s_0 = 0$ for $p = \{0, 2\}$ and $s_0 = L$ for $p = \{1, 3\}$. Defining $\varphi_2 = -\beta_2 L$, we obtain the expression of the amplitude of the output field on the trough port

$$B_T = k_2 K e^{j\varphi_2} \frac{[H_2 A_1^2 + \frac{\kappa_2}{D} (t_2^* A_5^2 + A_7^2 e^{-j\varphi_2})] + A_3^2 e^{-j\varphi_2}}{1 - t_2^* H_2 e^{2j\varphi_2}} \quad (4)$$

with

$$D = 1 - t_2^* \tau_2^* e^{2j\varphi_2}, \quad (5)$$

and where $H_2(2\omega)$ is the linear transfer function of the right microdisk for the SH field (see Fig. 1)

$$H_2 = \frac{\tau_2 - t_2^* e^{2j\varphi_2}}{1 - t_2^* \tau_2^* e^{2j\varphi_2}}. \quad (6)$$

For zinc-blende symmetry materials, the nonlinear coupling is characterized by

$$K = j \left[\chi_{0+}^{(2)} \frac{1 - e^{j\widetilde{\Delta\beta}_+ L}}{\widetilde{\Delta\beta}_+} + \chi_{0-}^{(2)} \frac{1 - e^{j\widetilde{\Delta\beta}_- L}}{\widetilde{\Delta\beta}_-} \right] \quad (7)$$

where the effective phase mismatch $\widetilde{\Delta\beta}_{\pm}$ is defined as

$$\widetilde{\Delta\beta}_{\pm} = \Delta\beta \pm \frac{2}{R}. \quad (8)$$

We apply the previous model to the case of two identical coupled GaP microdisks grown along the $z = [001]$ crystallographic axis and embedded in air as described in Fig. 2. The disks are separated by an air gap g , their thickness is $H = 136$ nm and their radius $R = 2.7$ μm . The properties of the system is obtained from the op-

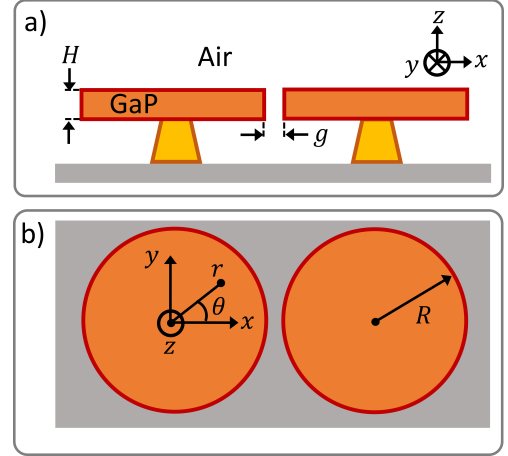


FIG. 2. Description of the structure numerically studied consisting of two GaP WGM microdisks embedded in air. a) side view and b) top view. g is the air gap separating the two disks, H and R are their thickness and radius.

tical properties of a single resonator. The confinement in the z -direction is taken into account using the effective index method (EIM) [29]. We used the lowest order guided modes in the z -direction both for the F and SH frequencies to optimize the effective nonlinear susceptibility. Due to the $\bar{4}3m$ symmetry of the GaP, the F field is chosen polarized in the (x, y) plan which gives an SH field polarized in the z -direction. Thus in the EIM framework, the F field is TE polarized whereas the SH field in TM polarized. The effective propagation constants calculated using this approximation are noted γ_1 and γ_2 respectively for the F and SF fields. The propagation constants β_1 and β_2 of the two modes are obtained solving the Helmholtz equation for a cylinder of refractive index $\gamma_{1,2}/k_0$ (with $k_0(\omega)$ the free space wavevector) surrounded by air. Note that for both frequencies we have chosen the modes with the lowest radial order to reach a good overlap of the interacting fields and thus a maximal effective non-linear susceptibility [11]. In this case it is not possible to use the modal phase matching technique to compensate for the dispersion to reach the phase matching condition. Figure 3.a) shows the linear transmission spectra for a single disk on the drop port assuming that the intrinsic and coupling quality (Q) factors are equal to 10^4 . ν_F is the F mode frequency, the frequency ν_{SH} of the SH field has been divided by two

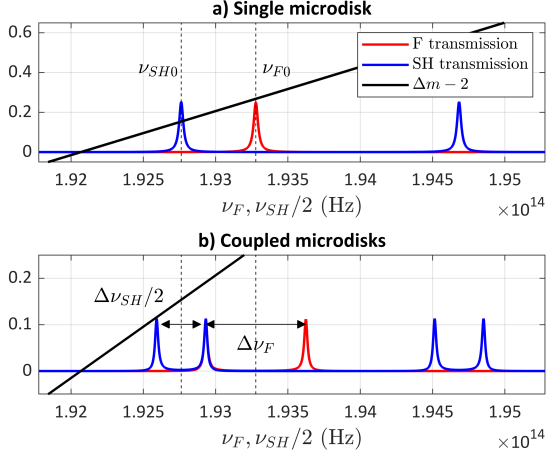


FIG. 3. Transmission spectra calculated on the drop port and azimuthal quantum number mismatch. a) for a single resonator the double resonance $\nu_{F0} = \nu_{SH0}/2$ and the condition $|\Delta m - 2| < 1/2$ can not be fulfilled due to the dispersion. b) By coupling the two disks it is possible to reach both conditions simultaneously.

for the sake of clarity. Due to the strong material and form dispersions it is not possible to reach the double resonance with a difference in the phase mismatch such as $\Delta m - 2 = 0$ (where $\Delta m = \Delta \beta R$ is the phase mismatch in term of azimuthal quantum numbers), consequently ν_{F0} and ν_{SH0} the resonant frequencies for the F and the SH modes giving a minimal phase mismatch do not coincide and $\nu_{F0} > \nu_{SH0}/2$. The double resonance $\nu_{F0} = \nu_{SH0}/2$ could be obtain but with $\Delta m - 2$ equal to an integer strictly positive which would lead to a null SHG over a circumference of the resonator. By coupling two identical resonators, the F and SH resonances are split by respectively $\Delta \nu_F$ and $\Delta \nu_{SH}$, values depending on g . If we define the new frequency mismatch between the split resonant frequencies

$$\delta(g) = \frac{\nu_{SH0}}{2} - \nu_{F0} - \frac{1}{2} \left(\Delta \nu_F(g) + \frac{\Delta \nu_{SH}(g)}{2} \right) \quad (9)$$

it is possible to find an air-gap value g_0 which makes the two inner F and SH frequencies to match reaching the phase matching as shown in Fig. 3.b). At the same time we have $|\Delta m - 2| < 1/2$ which insures an efficient SHG over the perimeter of each resonator. To find the value of g_0 we used a home-made FDTD code [30] to calculate the linear spectra around F and SH frequencies for the coupled structure for several values of g . Thus, the detuning δ can be calculated varying the air-gap as shown in Fig. 4.a). The corresponding coupling coefficients necessary to calculate the SHG in the coupled mode framework using Eq. (4) are deduced from $|\kappa_1| = \sin\left(\frac{\pi \Delta \nu_F}{\Delta_1}\right)$ and $|\kappa_2| = \sin\left(\frac{\pi \Delta \nu_{SH}}{\Delta_2}\right)$ where Δ_1 and Δ_2 are respectively the free spectral range (FSR) for the F and SH fields [31], the

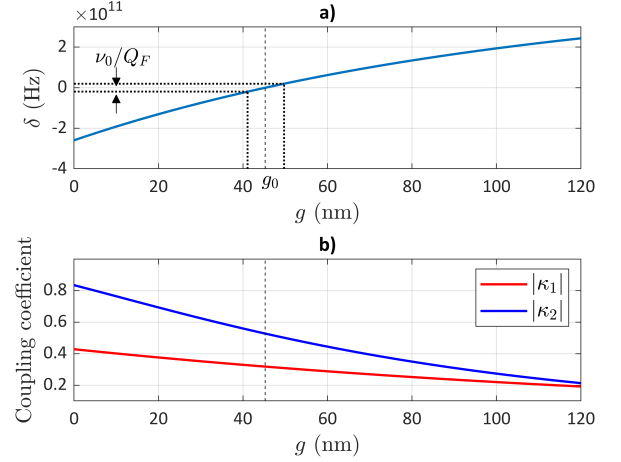


FIG. 4. a) Nonlinear detuning $\delta(g)$ calculated using a combinations of FDTD simulations and EIM. b) Coupling coefficients κ_1 and κ_2 deduced from FDTD simulations. The vertical dashed line gives the air gap value g_0 fulfilling the double resonance condition.

resulting values are plotted in Fig. 4.b). For a microdisk, the effective nonlinear susceptibilities is calculated for the single resonator WGM modes of resonant frequencies ν_{F0} and ν_{SH0} and azimuthal quantum numbers $m_1 = 17$ and $m_2 = 36$. Cylindrical coordinates (r, θ) are defined in Fig. 2 and $d_{14} = 28.5$ pm/V is the nonlinear coefficient of bulk GaP [32]. From the coupling mode theory [11] we find

$$\chi_{0\pm}^{(2)} = -\frac{j\gamma_2}{4R^2 N_2^2} \int_0^R r^2 d_{14} f_{\pm}(r) (\mathcal{H}_r^{SH})^* dr, \quad (10)$$

where N_2 is the bulk refractive index of GaP at the SH frequency. In expression (10) we have assumed that

$$f_{\pm}(r) = \mathcal{E}_r^F \mathcal{E}_\theta^F \pm j \frac{(\mathcal{E}_r^F)^2 - (\mathcal{E}_\theta^F)^2}{2}. \quad (11)$$

The F electric fields can be expressed using J_α the first kind Bessel functions of order α

$$\mathcal{E}_r^F = -\frac{am_1}{r\epsilon_0} \left(\frac{2\pi\nu_{F0}}{\gamma_1 c} \right)^2 J_{m_1}(\gamma_1 r) \quad (12)$$

and

$$\mathcal{E}_\theta^F = -\frac{j}{m_1} \frac{d(r\mathcal{E}_r^F)}{dr}. \quad (13)$$

Eventually, the SH magnetic field is given by

$$\mathcal{H}_r^{SH}(r) = b J_{m_2}(\gamma_2 r). \quad (14)$$

The constants a and b are calculated in order that $|\mathcal{A}_i|^2$ and $|\mathcal{B}_i|^2$ correspond to the power flows for the F and SH modes in W/m [11]. Figure 5 represents the normalized conversion efficiency $\eta = \frac{|B_T|^2}{|A_{in}|^2 P_{in}}$ for the studied

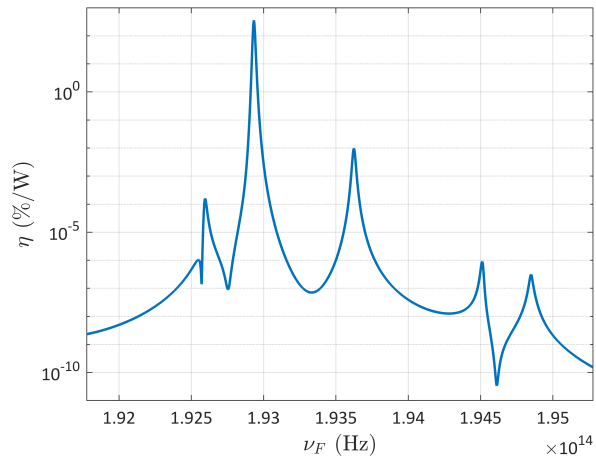


FIG. 5. Conversion efficiency $\eta(\nu_F)$ calculated for $\delta(g_0) = 0$.

structure in the case $g = g_0$. For the doubly resonant frequency we obtain a maximal conversion efficiency of 360%/W which is consistent with results calculated for small thin microdisks (with same Q-factors) under perfect phase matching [32]. This result shows that even though we obtained the double resonance with two supermodes with different symmetry it does not affect the efficiency of the device. The interest of the proposed method is that the resonator coupling gives an additional free parameter which would allow to use thicker and largest disks which would be less sensitive to fabrication imperfections. If we suppose a tolerance of ν_{F0}/Q_F (with Q_F the loaded Q-factor for the F) for the double reso-

nance in frequency it translates in a 10 nm fabrication tolerance for the air-gap. Note that the relative phase between the two coupling coefficients κ_1 and κ_2 has a negligible effect on the conversion efficiency maximum.

We have proposed a new method to reach the phase matching condition in second-order nonlinear processes in integrated optics relying on the use of the frequency splitting due to the coupling of identical resonators. We show how this phase matching scenario could be implemented using GaP microdisks to reach conversion yields such high as 360%/W with micron-size devices. The resonator coupling could also be used as the additional free parameter required to reach the double resonance condition in single mode nonlinear Fabry-Perot microcavities [33]. This method could be straightforwardly applied to a chain of three resonators which could be useful to reach higher frequency splittings for a given coupling strength between resonators enabling the compensation of larger phase-mismatch. Finally our approach could be profitably applied to the SHG in nano-resonators [34] such as coupled photonic crystal cavities. Indeed, since the splitting strongly depends on the FSR of the cavity, huge detuning as high as several nanometers could be canceled in these ultimately short cavities [35].

FUNDING INFORMATION

This research was supported by the French National Research Agency (ANR) through the JCJC Orpheus project (ANR-17-CE24-0019) and the "France 2030" OF-COC project (ANR-22-PEEL-0005).

-
- [1] G. Lin, A. Coillet, and Y. K. Chembo, "Nonlinear photonics with high-Q whispering-gallery-mode resonators," *Adv. Opt. Photon.* **9**, 828–890 (2017).
 - [2] B. Stern, X. Ji, Y. Okawachi, A. L. Gaeta, and M. Lipson, "Battery-operated integrated frequency comb generator," *Nature* **562**, 401 (2018).
 - [3] P. Liu, H. Wen, L. Shi, and X. Zhang, " $\chi^{(2)}$ nonlinear photonics in integrated microresonators," *Frontiers of Optoelectronics* **16**, 18 (2023).
 - [4] F. Baboux, G. Moody, and S. Ducci, "Nonlinear integrated quantum photonics with AlGaAs," *Optica* **10**, 917–931 (2023).
 - [5] Y. Wang, Z. Pan, Y. Yan, Y. Yang, W. Zhao, N. Ding, X. Tang, P. Wu, Q. Zhao, and Y. Li, "A review of gallium phosphide nanophotonics towards omnipotent nonlinear devices," *Nanophotonics* **13**, 3207–3252 (2024).
 - [6] A. Fiore, S. Janz, L. Delobel, P. van der Meer, P. Bravetti, V. Berger, E. Rosencher, and J. Nagle, "Second-harmonic generation at $\lambda=1.6 \mu\text{m}$ in AlGaAs/Al₂O₃ waveguides using birefringence phase matching," *Applied Physics Letters* **72**, 2942–2944 (1998).
 - [7] Y. Dumeige, I. Sagnes, P. Monnier, P. Vidakovic, I. Abram, C. Mériadeuc, and A. Levenson, "Phase-matched frequency doubling at photonic band edges: Efficiency scaling as the fifth power of the length," *Phys. Rev. Lett.* **89**, 043901 (2002).
 - [8] S. Ducci, L. Lanco, V. Berger, A. De Rossi, V. Ortiz, and M. Calligaro, "Continuous-wave second-harmonic generation in modal phase matched semiconductor waveguides," *Applied Physics Letters* **84**, 2974–2976 (2004).
 - [9] A. S. Helmy, "Phase matching using bragg reflection waveguides for monolithic nonlinear optics applications," *Opt. Express* **14**, 1243–1252 (2006).
 - [10] K. Pantzas, S. Combrié, M. Bailly, R. Mandouze, F. R. Talenti, A. Harouri, B. Gérard, G. Beaudoin, L. Le Gratiet, G. Patriarche, A. De Rossi, Y. Léger, I. Sagnes, and A. Grisard, "Continuous-wave second-harmonic generation in orientation-patterned gallium phosphide waveguides at telecom wavelengths," *ACS Photonics* **9**, 2032–2039 (2022).
 - [11] Y. Dumeige and P. Féron, "Whispering-gallery-mode analysis of phase-matched doubly resonant second-harmonic generation," *Phys. Rev. A* **74**, 063804 (2006).

- [12] A. Lorenzo-Ruiz and Y. Léger, “Generalization of second-order quasi-phase matching in whispering gallery mode resonators using berry phase,” *ACS Photonics* **7**, 1617–1621 (2020).
- [13] P. S. Kuo, J. Bravo-Abad, and G. S. Solomon, “Second-harmonic generation using quasi-phasematching in a GaAs whispering-gallery-mode microcavity,” *Nature Communications* **5**, 3109 (2014).
- [14] S. Mariani, A. Andronico, A. Lemaître, I. Favero, S. Ducci, and G. Leo, “Second-harmonic generation in AlGaAs microdisks in the telecom range,” *Opt. Lett.* **39**, 3062–3065 (2014).
- [15] D. P. Lake, M. Mitchell, H. Jayakumar, L. F. dos Santos, D. Curic, and P. E. Barclay, “Efficient telecom to visible wavelength conversion in doubly resonant gallium phosphide microdisks,” *Applied Physics Letters* **108**, 031109 (2016).
- [16] L. Chang, A. Boes, P. Pintus, J. D. Peters, M. Kennedy, X.-W. Guo, N. Volet, S.-P. Yu, S. B. Papp, and J. E. Bowers, “Strong frequency conversion in heterogeneously integrated GaAs resonators,” *APL Photonics* **4**, 036103 (2019).
- [17] C. Simonneau, J. P. Debray, J. C. Harmand, P. Vidaković, D. J. Lovering, and J. A. Levenson, “Second-harmonic generation in a doubly resonant semiconductor microcavity,” *Opt. Lett.* **22**, 1775–1777 (1997).
- [18] Z.-F. Bi, A. W. Rodriguez, H. Hashemi, D. Duchesne, M. Loncar, K.-M. Wang, and S. G. Johnson, “High-efficiency second-harmonic generation in doubly-resonant $\chi^{(2)}$ microring resonators,” *Opt. Express* **20**, 7526–7543 (2012).
- [19] Z. Lin, X. Liang, M. Lončar, S. G. Johnson, and A. W. Rodriguez, “Cavity-enhanced second-harmonic generation via nonlinear-overlap optimization,” *Optica* **3**, 233–238 (2016).
- [20] A. Armaroli, P. Féron, and Y. Dumeige, “Stable integrated hyper-parametric oscillator based on coupled optical microcavities,” *Opt. Lett.* **40**, 5622–5625 (2015).
- [21] X. Lu, Y. Sun, A. Chanana, U. A. Javid, M. Davanco, and K. Srinivasan, “Multi-mode microcavity frequency engineering through a shifted grating in a photonic crystal ring,” *Photon. Res.* **11**, A72–A79 (2023).
- [22] S. Sanyal, Y. Okawachi, Y. Zhao, B. Y. Kim, K. J. McNulty, M. Lipson, and A. L. Gaeta, “Nonlinear dynamics of coupled-resonator kerr combs,” *Phys. Rev. Lett.* **134**, 123801 (2025).
- [23] Y. Dumeige, L. Ghisa, and P. Féron, “Integrated all-optical pulse restoration with coupled nonlinear microring resonators,” *Opt. Lett.* **31**, 2187–2189 (2006).
- [24] Y. Xu, R. K. Lee, and A. Yariv, “Propagation and second-harmonic generation of electromagnetic waves in a coupled-resonator optical waveguide,” *J. Opt. Soc. Am. B* **17**, 387–400 (2000).
- [25] Y. Dumeige, “Miniaturization of fresnel phase matching using a side-coupled integrated spaced sequence of resonators (scissor),” *Opt. Lett.* **32**, 3438–3440 (2007).
- [26] Y. Dumeige, “Quasi-phase-matching and second-harmonic generation enhancement in a semiconductor microresonator array using slow-light effects,” *Phys. Rev. A* **83**, 045802 (2011).
- [27] A. Yariv, “Universal relations for coupling of optical power between microresonators and dielectric waveguides,” *Electronics Letters* **36**, 321–322 (2000).
- [28] Z. Yang, P. Chak, A. D. Bristow, H. M. van Driel, R. Iyer, J. S. Aitchison, A. L. Smirl, and J. E. Sipe, “Enhanced second-harmonic generation in AlGaAs microring resonators,” *Opt. Lett.* **32**, 826–828 (2007).
- [29] P. S. Kuo and G. S. Solomon, “On- and off-resonance second-harmonic generation in GaAs microdisks,” *Opt. Express* **19**, 16898–16918 (2011).
- [30] N. Jebali, L. Bodiou, J. Charrier, A. Armaroli, and Y. Dumeige, “Combining ftdt and coupled-mode theory for self-pulsing modeling in coupled nonlinear microring resonators,” *J. Opt. Soc. Am. B* **37**, 2557–2563 (2020).
- [31] D. D. Smith, H. Chang, and K. A. Fuller, “Whispering-gallery mode splitting in coupled microresonators,” *J. Opt. Soc. Am. B* **20**, 1967–1974 (2003).
- [32] P. Guillemé, M. Vallet, J. Stodolna, A. Ponchet, C. Cornet, A. Létoublon, P. Féron, O. Durand, Y. Léger, and Y. Dumeige, “Antiphase domain tailoring for combination of modal and $\bar{4}$ -quasi-phase matching in gallium phosphide microdisks,” *Opt. Express* **24**, 14608–14617 (2016).
- [33] V. Berger, “Second-harmonic generation in monolithic cavities,” *J. Opt. Soc. Am. B* **14**, 1351–1360 (1997).
- [34] F. Raineri, Y. Dumeige, A. Levenson, and X. Letartre, “Nonlinear decoupled ftdt code: phase-matching in 2d defective photonic crystal,” *Electronics Letters* **38**, 1704–1706 (2002).
- [35] S. Azzini, D. Grassani, M. Galli, D. Gerace, M. Patrini, M. Liscidini, P. Velha, and D. Bajoni, “Stimulated and spontaneous four-wave mixing in silicon-on-insulator coupled photonic wire nano-cavities,” *Applied Physics Letters* **103**, 031117 (2013).